

# Masked Feature Modeling Enhances Adaptive Segmentation

Wenlv Zhou, Zhiheng Zhou, Tiantao Xian, Yikui Zhai, Weibin Wu, Biyun MA

## Abstract

Unsupervised domain adaptation (UDA) for semantic segmentation aims to transfer models from a labeled source domain to an unlabeled target domain. While auxiliary self-supervised tasks—particularly contrastive learning—have improved feature discriminability, masked modeling approaches remain underexplored in this setting, largely due to architectural incompatibility and misaligned optimization objectives. We propose Masked Feature Modeling (MFM), a novel auxiliary task that performs feature masking and reconstruction directly in the feature space. Unlike existing masked modeling methods that reconstruct low-level inputs or perceptual features (e.g., HOG or visual tokens), MFM aligns its learning target with the main segmentation task, ensuring compatibility with standard architectures like DeepLab and DAFormer without modifying the inference pipeline. To facilitate effective reconstruction, we introduce a lightweight auxiliary module, Rebuilder, which is trained jointly but discarded during inference, adding zero computational overhead at test time. Crucially, MFM leverages the segmentation decoder to classify the reconstructed features, tightly coupling the auxiliary objective with the pixel-wise prediction task to avoid interference with the primary task. Extensive experiments across various architectures and UDA benchmarks demonstrate that MFM consistently enhances segmentation performance, offering a simple, efficient, and generalizable strategy for unsupervised domain-adaptive semantic segmentation.

## Introduction

Deep learning has achieved significant success in computer vision, including tasks such as semantic segmentation (Minaee et al. 2021). However, these models often struggle when faced with domain shift—a mismatch between training and testing data distributions—which can lead to notable performance degradation (Wang and Deng 2018). Addressing this issue by collecting and annotating new target domain data is resource-intensive and time-consuming, particularly for dense pixel-level annotations in semantic segmentation (Cordts et al. 2016; Sakaridis, Dai, and Van Gool 2021). Unsupervised domain adaptation (UDA) (Zhou and Zhou 2024) offers a practical alternative, enabling models to utilize labeled source domain data and unlabeled target

Copyright © 2026, Association for the Advancement of Artificial Intelligence (www.aaai.org). All rights reserved.

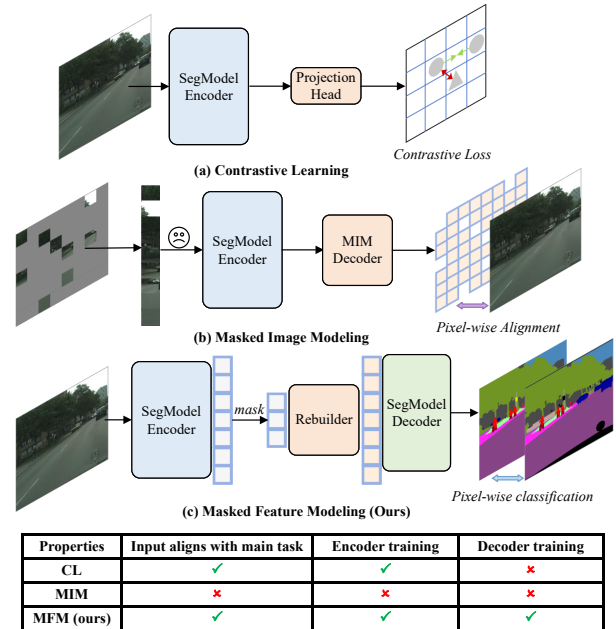


Figure 1: Comparison of three auxiliary tasks for UDA segmentation. (a) Contrastive Learning (CL) uses contrastive loss for feature alignment but does not involve training the decoder, limiting end-to-end model optimization. (b) Masked Image Modeling (MIM) reconstructs masked component but disrupts the input pipeline, reducing compatibility with certain architectures. (c) Masked Feature Modeling (MFM) performs masking and reconstruction in the feature space, aligns with the segmentation task, remains compatible with diverse architectures, and improves performance without incurring inference overhead, as the Rebuilder is used only during training.

domain data to improve performance without additional annotation efforts.

Auxiliary tasks provide a promising direction for enhancing UDA-based segmentation models (Xie et al. 2023; Chen et al. 2023; Tsai et al. 2018; Hoyer et al. 2023b). These tasks, typically designed to require no manual annotations and to integrate seamlessly with existing architectures, enrich feature representations without disrupting the

primary network. Among them, contrastive learning (Chen et al. 2020; He et al. 2020) has shown strong potential by improving feature discrimination: pulling similar samples closer while pushing dissimilar ones apart (Figure 1(a)). This makes it particularly useful for UDA segmentation, where distinguishing challenging categories is critical (Xie et al. 2023; Chen et al. 2023; Lee et al. 2022; Li et al. 2023; Chen et al. 2024). However, another self-supervised technique—masked image modeling (MIM)—has seen limited exploration in the context of UDA segmentation. MIM methods, such as masked autoencoders (MAE) (He et al. 2022), train models to reconstruct occluded regions, fostering a better understanding of global context and scene structure. While this approach seems suitable for UDA segmentation by encouraging models to capture broader scene context, its adoption is limited. We speculate that this mainly stems from two main challenges:

(i) *Input structure constraints*: MIM modifies the input structure by masking image patches (Figure 1(b)), complicating its application to segmentation networks like DeepLab (L. Chen, G. Papandreou, I. Kokkinos, K. Murphy and A. Yuille 2017) or DAFormer (Hoyer, Dai, and Van Gool 2022).

(ii) *Optimization conflicts*: MIM methods focus on element-wise reconstructing occluded patches, which may introduce conflicts with the optimization objectives of domain adaptive segmentation tasks.

To address these challenges, we propose Masked Feature Modeling (MFM), a novel auxiliary task specifically designed for UDA segmentation, see Figure 1(c). By performing masking and reconstruction in the feature space rather than the image space, MFM avoids disruptions to the input paradigm, making it compatible with a wide range of architectures, including CNNs (L. Chen, G. Papandreou, I. Kokkinos, K. Murphy and A. Yuille 2017) and Transformers (Hoyer, Dai, and Van Gool 2022). Additionally, MFM ensures that its optimization objectives align with the primary segmentation task by using the segmentation decoder to perform pixel-wise classification on the completed features, rather than treating pixel-wise alignment as the optimization objective. This design minimizes conflicts between auxiliary and primary tasks while uniquely enhancing the decoder, a benefit not typically offered by contrastive learning (Chen et al. 2020; He et al. 2020). To achieve feature completion, similar to the paradigm of MIM (He et al. 2022; Assran et al. 2023; Wang et al. 2023; Woo et al. 2023), we also introduce an asymmetric and lightweight auxiliary module, named Rebuilder, to facilitate masked feature reconstruction. During training, the Rebuilder is jointly trained with the segmentation network and is removed after training, ensuring no additional inference cost. This approach allows MFM to improve domain adaptation performance efficiently and effectively.

In summary, our contributions are as follows:

(i) We propose Masked Feature Modeling (MFM), an auxiliary task that performs feature-level masking and reconstruction, addressing limitations of image-based MIM methods for UDA segmentation.

(ii) We introduce the Rebuilder, a lightweight auxiliary

module that aligns auxiliary and main task objectives, integrates seamlessly with segmentation models, and is discarded at inference to eliminate additional overhead.

(iii) Through extensive experiments, we demonstrate MFM’s effectiveness across diverse UDA benchmarks, highlighting its compatibility with various architectures and its ability to achieve competitive performance.

## Related Work

**Semantic segmentation**, a cornerstone of computer vision, has seen significant progress with deep learning. Fully Convolutional Networks (FCNs) (Long, Shelhamer, and Darrell 2015) enabled pixel-level understanding, but challenges like small object delineation and complex scenes persist. The encoder-decoder architecture improved segmentation with innovations like skip-connections (Ronneberger, Fischer, and Brox 2015) for feature fusion and dilated convolutions (Chen et al. 2018) to expand receptive fields. While CNN-based methods dominated early research, Transformers (Zheng et al. 2021; Xie et al. 2021; Cheng et al. 2022) have advanced global context modeling. Despite their performance, Transformers’ self-attention mechanism is computationally intensive for high-resolution images (Vaswani et al. 2017). Xie *et al.* (Xie et al. 2021) mitigated this by downsampling key and value components in self-attention.

**Unsupervised domain adaptive segmentation** addresses the challenge of adapting segmentation models to new domains without target annotations. Common approaches include adversarial training (Tsai et al. 2018; Hoffman et al. 2018), self-training (Tranheden et al. 2021; Zou et al. 2018), and efficient architecture design (Hoyer, Dai, and Van Gool 2022, 2024). Beyond these, auxiliary tasks have been introduced to enhance feature representation: contrastive learning improves backbone features (Xie et al. 2023; Chen et al. 2023), while depth estimation aids scene understanding (Hoyer et al. 2023b). Though effective, these methods typically focus on the encoder and may conflict with the main task. Our method, MFM, overcomes these limitations by training the entire model, aligning encoder and decoder under the same objective to reduce potential conflicts.

**Masked image modeling** learn representations from images corrupted by masking. The concept of using masking for representation learning has its roots in image inpainting, with Context Encoders (Pathak et al. 2016) using convolutional networks to inpaint large masked regions. Recent methods leverage ViT (Dosovitskiy et al. 2021) explores masked patch prediction for self-supervised learning. BEiT (Bao et al. 2022) extends the idea by predicting discrete tokens, similar to masked language modeling. MAE (He et al. 2022) further advance this direction by masking large portions of the image and using transformers for efficient pre-training. On the other hand, ConvNextv2 (Woo et al. 2023) proposes a convolutional variant of masked autoencoders, demonstrating that convolutional architectures can be effective for MIM. MIM enables efficient representation learning but faces challenges as an auxiliary task. Masking input patches disrupts the data-processing paradigm of the original pipeline, and methods like MAE (He et al. 2022) are

hard to adapt to Deeplab (L. Chen, G. Papandreou, I. Kokkinos, K. Murphy and A. Yuille 2017) and DAFormer (Hoyer, Dai, and Van Gool 2022). To address this, we propose MFM, which masks and reconstructs in the feature space, preserving the input paradigm and supporting diverse architectures.

## Method

### Preliminary

**Unsupervised domain adaptive segmentation** aims to train a neural network using labeled source domain data  $D_s = \{(x_k^s, y_k^s)\}_{k=1}^{n_s}$  to perform well on a target domain  $D_t = \{(x_k^t)\}_{k=1}^{n_t}$ , without access to target labels. In semantic segmentation model (SegModel), typically consists of an Encoder  $E(\cdot)$  and a Decoder  $D(\cdot)$ . Simply training the network using pixel-wise cross-entropy on the source domain can be formulated as:

$$\mathcal{L}_{sup} = - \sum_{i=1}^H \sum_{j=1}^W \sum_{c=1}^C y_{ijc}^s \log D(E(x^s))_{ijc} \quad (1)$$

where  $H$  and  $W$  represent the image’s height and width respectively, while  $C$  signifies the number of categories in the UDA task.

However, a model trained solely on the source domain often experiences a performance decline when applied to a different domain. To address this issue, UDA methods leverage unlabeled target domain images to adapt the network. To achieve this, an additional unsupervised loss  $\mathcal{L}_{uda}$  is introduced into the optimization process.

$$\mathcal{L}_{overall} = \mathcal{L}_{sup} + \mathcal{L}_{uda} \quad (2)$$

**Masked image modeling** is a self-supervised learning paradigm designed to train neural networks by reconstructing masked portions of an input image. The input image  $x$  is reshaped into non-overlapping patches  $p = \{p_i\}_{i=1}^{N_t}$ . MIM constructs a random mask  $M^{mim} \in \{0, 1\}^{N_t}$  to indicate the masked patches, where  $M_i^{mim} = 1$  corresponds to the patches that are masked. Only the visible patches  $p^v = \{p_i \mid M_i^{mim} = 0\}_{i=1}^{N_v}$  are fed into the encoder and are mapped to potential features, after which a lightweight decoder  $D_{mim}$  is introduced to reconstruct the pixel values of the invisible patches.

$$\mathcal{L}_{mim} = - \sum_{i=1}^{N_i} M_i^{mim} \cdot (D_{mim}(E(p_i^v)) - p_i)^2 \quad (3)$$

Incorporating MIM as an auxiliary task poses challenges since typical UDA segmentation architectures (L. Chen, G. Papandreou, I. Kokkinos, K. Murphy and A. Yuille 2017; Hoyer, Dai, and Van Gool 2022) are designed to process complete images rather than visible patches.

### Masked Feature Modeling

Masked Feature Modeling (MFM) is a simple approach designed to address the limitations of mainstream MIM methods when used as an auxiliary task. Unlike MIM, MFM

eliminates the need for the SegModel encoder  $E(\cdot)$  to process partially visible signals. Instead, it reconstructs the original signal from the partially visible features provided to the encoder. The SegModel decoder  $D(\cdot)$  then processes the reconstructed signal, and the model is trained through a pixel-wise classification task.

$$\mathcal{L}_{mfm} = - \sum_{i=1}^H \sum_{j=1}^W \sum_{c=1}^C \tilde{y}_{ijc} \log D(R(E(x^t)))_{ijc} \quad (4)$$

Here,  $\tilde{y}$  is the pseudo label (Lee et al. 2013) of target image, and  $R(\cdot)$  represents the Rebuilder (refer to next section for detailed information), whose role is analogous to the lightweight decoder in MIM (He et al. 2022; Woo et al. 2023). Both are responsible for reconstructing the original signal from partially visible signals. When the MFM task is used as an auxiliary task for unsupervised domain adaptive segmentation, the overall optimization objective can be expressed as:

$$\mathcal{L}_{overall} = \mathcal{L}_{sup} + \mathcal{L}_{uda} + \lambda \mathcal{L}_{mfm} \quad (5)$$

where  $\lambda$  is the trade-off in masked feature modeling. MFM can be easily integrated with existing UDA methods.

### Rebuilder

The Rebuilder  $R(\cdot)$  primarily serves to randomly mask out certain SegModel encoder feature regions and then reconstruct them. Its design is largely consistent with the decoder (He et al. 2022; Wang et al. 2023; Assran et al. 2023; Bardes et al. 2024) used in MIM. After the semantic segmentation model has been fully trained, the Rebuilder is removed, ensuring it does not impact the inference process of the original model. The pipeline of the Rebuilder is shown in Figure 2, and the following sections will discuss the specific design details. See **Supplementary Material** for further details and pluggable analysis.

**Feature embedding.** Since different encoders (L. Chen, G. Papandreou, I. Kokkinos, K. Murphy and A. Yuille 2017; Hoyer, Dai, and Van Gool 2022) produce features at varying scales, it is essential to ensure that subsequent transformer blocks can efficiently process the features from different encoders in a consistent manner. Thus, the input feature  $f^t = E(x^t)$ ,  $f^t \in \mathbb{R}^{C \times H \times W}$  is scaled to  $C' \times H' \times W'$  to obtain embedding feature  $\tilde{f}^t$ . For the channel dimension, a linear mapping layer is applied for rescaling. After processing the channel dimension, bilinear interpolation is used to resize the input feature to the target spatial dimensions when the input and target spatial dimensions are not aligned.

**Masking.** Based on the shape of the features obtained after feature embedding, a binary mask  $M \in \mathbb{R}^{H' \times W'}$  is generated through uniform random sampling (He et al. 2022). We apply the generated mask to perform masked out operation on the embedding features, and fill the corresponding positions of the removed features with a mask token. Each mask token (Kenton and Toutanova 2019) is a shared, learnable vector that represents the presence of a missing

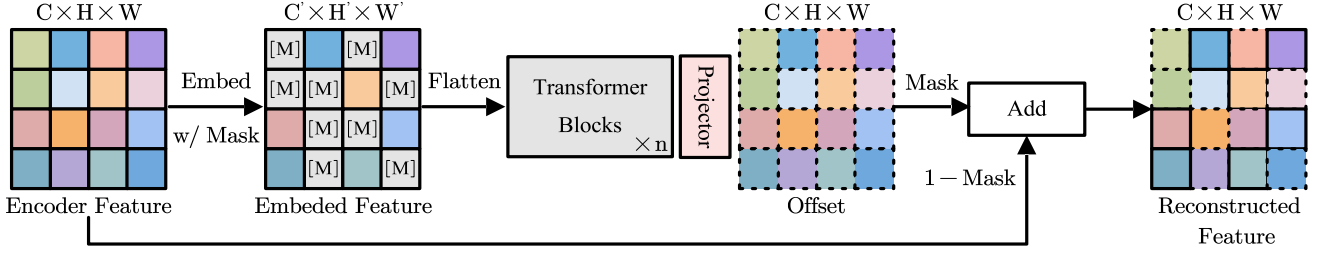


Figure 2: The pipeline of Rebuilder. The Rebuilder is designed to randomly mask out features from the encoder and reconstruct the masked component. It first scales the encoder features along both spatial and channel dimensions, and then applies random masking to remove a subset of these features. Subsequently, the masked features are passed through several Transformer blocks and a projector to generate reconstructed features, which are input to the decoder for model training. [M] is a learnable token.

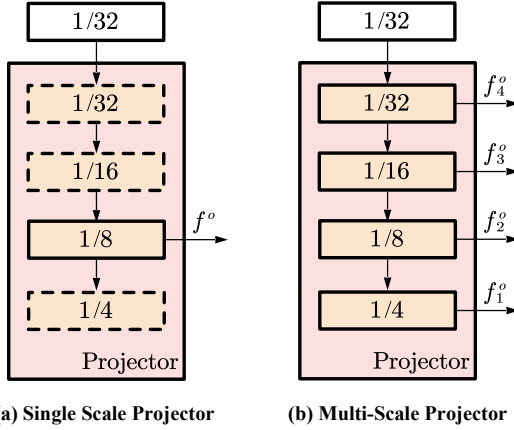


Figure 3: An overview of the projector. The features from the Transformer are reshaped and fed into the projector, which uses several transposed convolutions to generate features at different scales. (a) The single-scale projector and (b) the multi-scale projector are used for MFM training in single-scale models (e.g., DeepLab-V2) and multi-scale models (e.g., DAFormer), respectively.

patch to be predicted. The processed features are reshaped to  $(H'W') \times C'$  and fed into the subsequent parts of the architecture.

**Architecture.** Since the mask token lacks positional information, following works (He et al. 2022; Wang et al. 2023; Assran et al. 2023; Bardes et al. 2024) the reshaped features are first added with absolute positional embeddings (Vaswani et al. 2017). A series of Transformer blocks  $T(\cdot)$  (Dosovitskiy et al. 2021) are then applied to process these features. Experiment demonstrate that MFM achieves performance gains with only a minimal number of blocks (e.g.,  $n = 1$  or  $n = 2$ ), thus avoiding significant computational overhead, details in Table 2(b). In addition, a projector  $P(\cdot)$  is used to map the Transformer’s output features to the original feature map dimensions. The projector consists of transposed convolution layers that rescale both spatial and channel dimensions to align with the original feature, as shown in Figure 3(a).

After obtaining the offset  $f^o$  from the Projector’s output, the mask is resized to the original feature map size to obtain  $M^s \in \mathbb{R}^{H \times W}$ . Based on  $M^s$ , the offset features are fused with the original feature  $f^t$  to obtain the final reconstructed features  $f^r$ , where broadcasting is applied due to the channel dimension mismatch between the mask and feature tensors.

$$f^r = M^s \odot f^o + (1 - M^s) \odot f^t \quad (6)$$

where  $\odot$  is Hadamard product.

**Implemented with multi-scale model.** For the multi-scale model (e.g., DAFormer (Hoyer, Dai, and Van Gool 2022)) implementation, we do not create a Rebuilder with each stage. Due to the presence of the Transformer, such a straightforward design would introduce significant computational overhead. We adopt a simple approach by directly using the features from the last stage for feature embedding and Transformer processing. Specifically, we introduce a multi-scale projector, as shown in Figure 3(b). The structure of the multi-scale projector is almost identical to that of the single-scale projector, with the key difference being that the former uses the features after each transposed convolution as offset at different stages. Therefore, for multi-scale architectures like DAFormer (Hoyer, Dai, and Van Gool 2022), the MFM does not incur additional computational overhead. The feasibility of this approach is validated by ViTDet (Li et al. 2022), which successfully demonstrates that Transformer models can generate multi-scale features through transposed convolutions using only the features from the final stage. Given a hierarchical feature map  $f_i^t$ , where  $i \in \{1, 2, 3, 4\}$ , the corresponding reconstructed feature is:

$$f_i^r = M_i^s \odot f_i^o + (1 - M_i^s) \odot f_i^t \quad (7)$$

## Experiments

In this section, we focus on experimenting with two popular benchmarks: GTA  $\rightarrow$  Cityscape and Synthia  $\rightarrow$  Cityscape. First, we introduce the dataset along with the implementation details. Then, we compare our approach with state-of-the-art (SoTA) methods. Next, we explore the performance impact under various parameter settings through ablation studies.

Method	Road	S.walk	Build.	Wall	Fence	Pole	Tr.Light	Sign	Veget.	Terrain	Sky	Person	Rider	Car	Truck	Bus	Train	M.bike	Bike	mIOU
GTA → Cityscape																				
PiPa	96.1	72.0	90.3	56.6	52.0	55.1	61.8	63.7	90.8	52.6	93.6	74.3	43.6	93.5	78.4	84.2	77.3	59.9	66.7	71.7
GANDA	96.5	74.8	91.4	61.7	57.3	59.2	65.4	68.8	91.5	49.9	<b>94.7</b>	79.6	54.8	94.1	81.3	86.8	74.6	64.8	68.2	74.5
QuadMix	97.5	<b>80.9</b>	91.6	62.3	<b>57.6</b>	58.2	64.5	71.2	91.7	52.3	94.3	80.0	55.9	<b>94.6</b>	86.3	90.5	82.3	65.1	68.1	76.1
DACS	89.9	39.7	87.9	30.7	39.5	38.5	46.4	52.8	88.0	44.0	88.8	67.2	35.8	84.5	45.7	50.2	0.0	27.3	34.0	52.1
w/ MFM (ours)	94.7	68.3	87.6	38.1	27.4	42.0	51.9	59.2	86.9	45.0	87.7	66.3	32.3	89.6	53.9	56.6	0.0	33.2	42.1	55.9
DAFormer	95.7	70.2	89.4	53.5	48.1	49.6	55.8	59.4	89.9	47.9	92.5	72.2	44.7	92.3	74.5	78.2	65.1	55.9	61.8	68.3
w/ MFM (ours)	96.8	76.3	89.5	55.7	50.3	50.9	58.2	62.2	90.0	50.1	91.1	73.8	48.2	92.3	77.3	80.4	71.6	56.3	64.0	70.3
HRDA	96.4	74.4	91.0	61.6	51.5	57.1	63.9	69.3	91.3	48.4	94.2	79.0	52.9	93.9	84.1	85.7	75.9	63.9	67.5	73.8
w/ MFM (ours)	97.0	78.3	90.9	59.5	52.8	60.4	66.6	72.4	<b>91.9</b>	51.8	94.3	79.3	55.5	94.4	84.4	87.9	82.7	65.4	68.2	75.4
MIC	97.4	80.1	91.7	61.2	56.9	59.7	66.0	71.3	91.7	51.4	94.3	79.8	56.1	<b>94.6</b>	85.4	90.3	80.4	64.5	68.5	75.9
w/ MFM (ours)	<b>98.3</b>	80.4	<b>92.6</b>	<b>62.7</b>	57.0	<b>62.3</b>	<b>69.1</b>	<b>74.3</b>	91.8	<b>53.5</b>	<b>94.7</b>	<b>81.1</b>	<b>56.6</b>	94.1	<b>87.2</b>	<b>91.6</b>	<b>85.4</b>	<b>66.3</b>	<b>71.3</b>	<b>77.5</b>
Synthia → Cityscape																				
PiPa	87.9	48.9	88.7	45.1	4.5	53.1	59.1	58.8	87.8	-	92.2	75.7	49.6	88.8	-	53.5	-	58.0	62.8	63.4
GANDA	89.1	50.6	<b>89.7</b>	<b>51.4</b>	6.7	59.4	<b>66.8</b>	57.7	86.7	-	93.8	80.6	56.9	<b>90.7</b>	-	64.8	-	62.6	65.0	67.0
QuadMix	88.1	51.2	88.9	46.7	7.9	58.6	64.7	<b>63.7</b>	88.1	-	93.9	81.3	56.6	90.3	-	<b>66.9</b>	-	66.8	<b>66.0</b>	67.5
DACS	80.6	25.1	81.9	21.5	2.9	37.2	22.7	24.0	83.7	-	90.8	67.6	38.3	82.9	-	38.9	-	28.5	47.6	48.3
w/ MFM (ours)	83.5	44.2	84.9	21.5	3.4	41.6	47.2	52.3	83.7	-	86.5	68.6	42.1	84.1	-	51.2	-	40.4	58.2	55.8
DAFormer	84.5	40.7	88.4	41.5	6.5	50.0	55.0	54.6	86.0	-	89.8	73.2	48.2	87.2	-	53.2	-	53.9	61.7	60.9
w/ MFM (ours)	88.4	51.4	88.8	41.2	<b>8.4</b>	50.2	55.9	52.9	85.8	-	88.5	73.0	47.6	87.2	-	63.1	-	57.8	61.4	62.6
HRDA	85.2	47.7	88.8	49.5	4.8	57.2	65.7	60.9	85.3	-	92.9	79.4	52.8	89.0	-	64.7	-	63.9	64.9	65.8
w/ MFM (ours)	<b>90.6</b>	<b>55.5</b>	88.3	49.8	7.0	57.8	65.6	56.6	87.9	-	93.9	79.6	53.2	89.1	-	65.1	-	<b>67.8</b>	<b>66.0</b>	67.1
MIC	86.6	50.5	89.3	47.9	7.8	59.4	66.7	63.4	87.1	-	94.6	81.0	58.9	90.1	-	61.9	-	67.1	64.3	67.3
w/ MFM (ours)	87.5	53.2	<b>89.7</b>	48.7	7.8	<b>61.0</b>	66.7	63.1	<b>88.6</b>	-	<b>94.7</b>	<b>81.8</b>	<b>59.7</b>	90.1	-	64.3	-	<b>67.8</b>	65.3	<b>68.1</b>

Table 1: Comparison with state-of-the-art methods for UDA. The best result in each metric column is marked bold.

## Experiment Setups

**Dataset.** The GTA (Richter et al. 2016) dataset comprises 24,966 synthetic images featuring pixel-level semantic annotations. These images are generated within the open-world environment of “Grand Theft Auto V”, all captured from the perspective of a vehicle navigating the streets of American-style virtual cities. This dataset encompasses 19 semantic classes that align with those found in the Cityscapes dataset.

SYNTHIA (Ros et al. 2016) constitutes a synthetic urban scene dataset. We opt for its subset known as “SYNTHIA-RAND-CITYSCAPES”, which shares 16 common semantic annotations with Cityscapes. Specifically, we utilize a total of 9,400 images, each with a resolution of 1280×760, sourced from the SYNTHIA dataset.

Cityscapes (Cordts et al. 2016) is a dataset featuring real urban scenes captured across 50 cities in Germany and neighboring regions. The dataset includes meticulously annotated images, comprising 2,975 training images, 500 validation images, and 1,525 test images, all at a resolution of 2048×1024 pixels. Each pixel within these images is classified into one of 19 distinct categories.

**Baseline methods.** We select popular UDA segmentation methods such as DACS (Tranheden et al. 2021), DAFormer (Hoyer, Dai, and Van Gool 2022), HRDA (Hoyer, Dai, and Van Gool 2024), and MIC (Hoyer et al. 2023a) as baselines to validate the performance improvement of MFM on these baselines. We also compare our method with popular approaches such as QuadMix (Zhang et al. 2025), PiPa (Chen

et al. 2023), and GANDA (Liao et al. 2024).

**Implementation details.** To ensure fairness and reproducibility, the hyperparameters related to the Baselines are kept consistent with those in the original paper. For network architecture, we utilize the DeepLab-V2 (L. Chen, G. Papandreou, I. Kokkinos, K. Murphy and A. Yuille 2017) with ResNet101 (He et al. 2016) and DAFormer (Hoyer, Dai, and Van Gool 2022) with MiT-B5 (Xie et al. 2021) as the architecture.

For Masked Feature Modeling, we chose a trade-off  $\lambda$  value of 1.0. Regarding the design of the Rebuilder, the number of transformer blocks is set to 2, and the embedding dimension is set to 512. In the Feature Embedding section, we choose to scale the spatial and channel dimensions of the feature map, specifically setting  $H' = W' = 16$  and  $C' = 512$ . We set the masking ratio to 40%. The learning rate of  $6 \times 10^{-5}$  is employed with the Rebuilder. For the HRDA head (Hoyer, Dai, and Van Gool 2024), the MFM is trained using both the fused multi-scale predictions and the detail crop predictions, following the methodology described in the original paper. The results are averaged over 3 random seeds. All the experiments are conducted with 1x NVIDIA GTX 3090 with 24G RAM and the PyTorch framework is implemented to perform our experiments.

## Comparisons with State-of-the-Arts UDA Methods

We evaluate our method against state-of-the-art UDA approaches on two widely used benchmarks: GTA5 → Cityscapes and SYNTHIA → Cityscapes, using a vari-

ety of base learners, including DACS, DAFormer, HRDA, and MIC. As shown in Table 1, integrating the proposed MFM module leads to consistent performance improvements across all settings.

On the GTA5  $\rightarrow$  Cityscapes benchmark, MFM yields notable gains: +3.8 mIoU for DACS, +2.0 mIoU for DAFormer, +1.6 mIoU for HRDA, and +1.6 mIoU for MIC. The improvement is particularly pronounced in fine-grained categories such as traffic sign, rider, and motorbike, suggesting that MFM may enhance the decoder’s capacity for high-level semantic discrimination. In particular, the MIC + MFM combination achieves an mIoU of 77.5, which surpasses previous state-of-the-art results by a margin of +1.4.

Similarly, on the more challenging SYNTHIA  $\rightarrow$  Cityscapes benchmark, MFM consistently improves performance: +7.5 mIoU for DACS, +1.7 for DAFormer, +1.3 for HRDA, and +0.8 for MIC. These results suggest that MFM generalizes well across different adaptation strategies and datasets.

Overall, the findings indicate that MFM serves as a model-agnostic, plug-and-play auxiliary task that can complement existing UDA pipelines by more effectively aligning feature learning with semantic segmentation objectives.

### Ablation Study

In the ablation study, we use the DACS (Tranheden et al. 2021) as the baseline and DeepLab-V2 (L. Chen, G. Papandreou, I. Kokkinos, K. Murphy and A. Yuille 2017) with ResNet101 (He et al. 2016) as the network architecture to explore performance under different settings on the GTA  $\rightarrow$  Cityscape benchmark. Additional explorations can be found in the **Supplementary Material**.

**Masking ratio.** Figure 4 shows the model’s performance under different masking ratios. Unlike previous findings in MIM research, MFM achieves better performance at lower masking ratios. (With MAE (He et al. 2022) set to 75% and ConvNextv2 (Woo et al. 2023) set to 60%). The optimal performance is achieved when the masking ratio is 40%, reaching 55.9 mIoU, which is an improvement of +3.8 mIoU over the baseline.

We speculate that an excessively high masking ratio reduces the richness of the reconstructed features, causing similar features to be assigned to different class semantics, which degrades the model’s performance. While methods like MIM use higher masking ratios, their visible patches are processed by a powerful encoder that performs extensive contextual learning. In contrast, MFM’s visible patches are only learned by a few Transformer blocks, making a lower masking ratio more effective.

**Rebuilder design.** The architecture of Rebuilder is simple yet lightweight, a characteristic that allows MFM to serve as an auxiliary task without introducing significant additional training overhead. The specific design details can be found in Tables 2(a), 2(b), and 2(d).

The results demonstrate that a more powerful Rebuilder and longer token sequences lead to improved performance. The model achieves optimal performance when the embedding dimension is set to 512, the number of Transformer

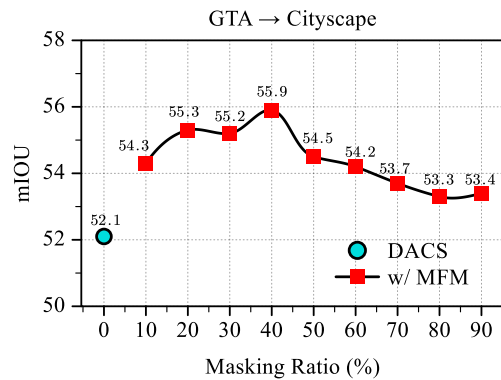


Figure 4: Masking ratio. The optimal performance enhancement is achieved when the masking ratio is adjusted to 40%.

blocks is 2, and  $H' = W' = 16$ . Even with just a single Transformer block, MFM still demonstrates a significant performance improvement.

However, as both the Rebuilder and sequence length are further scaled, the model’s performance sharply declines. This degradation can be attributed to the difficulty of training a Transformer model from scratch on top of a pre-trained model, which often results in instability during training. In contrast, reducing the capacity of the Rebuilder stabilizes the training process and yields better performance. However, this should not be interpreted as diminishing the importance of scaling the Rebuilder. In MIM-based research, stronger Transformer blocks consistently achieve better performance. For instance, in MAE (He et al. 2022), the number of Transformer blocks is set to 8, and in iJepa (Assran et al. 2023), it is set to 12. Therefore, future work should explore strategies to design a more powerful Rebuilder for auxiliary training.

**Masking and rebuilding contribution.** Since there are many masking-related regularization techniques in deep learning, such as Dropout (Srivastava et al. 2014) and DropBlock (Ghiasi, Lin, and Le 2018), we aim to explore how masking “ $(1 - M^s) \odot f^t$ ” and rebuilding “ $M^s \odot f^o$ ” in MFM contribute to performance improvement.

In Table 2(c), we observe that using masking alone even leads to a performance drop, with a -0.2 mIoU decrease compared to the baseline. This indicates that a large proportion of masking in the feature space causes an irreversible loss of semantic information, which the decoder alone cannot recover. However, with the addition of rebuilding, the performance improves significantly.

**Training objective.** We argue that the choice of training objective is crucial to the effectiveness of MFM. In masked modeling, the core task is to reconstruct hidden content—be it pixels in MAE (He et al. 2022), HOG descriptors in MaskFeat (Wei et al. 2022), or features in the JEPa series (Assran et al. 2023; Bardes et al. 2024). However, we find these typical reconstruction strategies suboptimal for MFM.

To investigate, we compare several common objectives using the same Rebuilder and training settings in Table 2(e). Pixel reconstruction with normalization, as in MAE, results

Dim	128	256	512	768
mIOU	54.7	55.1	<b>55.9</b>	53.6

(a) Embedding dimensions of Transformer blocks in the Rebuilder.

$H' = W'$	8	16	32	64
mIOU	55.6	<b>55.9</b>	54.1	OOM

(d) Spatial dimensions of the rescaled features. OOM marks out-of-memory.

Blocks	1	2	4	8
mIOU	55.4	<b>55.9</b>	54.4	52.9

(b) Number of Transformer blocks used in the Rebuilder.

Case	mIOU
Baseline	52.1
pixel rec. (w/ norm)	51.8
feature rec. (w/ teacher)	53.5
feature rec. (w/o teacher)	53.7
pixel cls.	<b>55.9</b>

(e) Training objective. Consistent objectives boost performance.

Case	mIOU
Baseline	52.1
Masking	51.9
Masking + Rebuilding	<b>55.9</b>

(c) Effect of masking and rebuilding on performance.

$\lambda$	0.1	0.5	1.0	2.0	10.0
mIOU	54.7	55.8	<b>55.9</b>	55.4	52.1

(f) Influence of the loss weight  $\lambda$  on performance.

Table 2: Ablation study of MFM using DeepLab-V2 with ResNet-101 on the GTA  $\rightarrow$  Cityscape benchmark with DACS.

in a -0.3 mIoU drop, likely due to its low-level nature being misaligned with the high-level semantics required for segmentation. To better match task semantics, we explore reconstructing high-level features. Inspired by iJEPa, we first adopt a teacher-based feature reconstruction strategy using the EMA teacher from DACS (Tranheden et al. 2021), which yields a slight improvement. A variant that reconstructs the student’s own features performs similarly.

Notably, when we replace reconstruction with direct pixel-wise classification using cross-entropy loss (“Pixel cls.”), the performance improves significantly, surpassing all other objectives. These results highlight a key principle in multi-task learning (Liebel and Körner 2018): auxiliary tasks are most effective when closely aligned with the main objective.

**Trade-off.** We also investigate the trade-off in Table 2(f). Surprisingly, the model’s performance is not sensitive to the trade-off setting, achieving similar performance gains across different configurations without requiring careful hyperparameter tuning. When the trade-off is set to 10, the model’s performance degrades, whereas the greatest improvement over the baseline is achieved at a trade-off value of 1.0.

## Limitations and Future Work

While MFM demonstrates strong performance across diverse architectures and datasets, several limitations remain:

- **Limited capacity of Rebuilder:** To maintain lightweight design, the Rebuilder employs only a small number of Transformer blocks. Although sufficient for current benchmarks, its ability to model complex feature dependencies may be limited in more diverse domains.
- **Training stability:** We observed that scaling up the Rebuilder or increasing the masking ratio can lead to unstable training. This reflects the difficulty of integrating auxiliary Transformer components with pre-trained segmentation models.

- **Task specificity:** MFM is specifically designed for pixel-wise classification tasks. Its direct extension to other dense prediction tasks such as depth estimation or panoptic segmentation requires further investigation.

In future work, we aim to explore more powerful and stable Rebuilder architectures, potentially leveraging pre-trained or distilled representations to improve semantic reconstruction, as well as incorporating diverse masking strategies to enhance robustness. Moreover, we plan to generalize the MFM paradigm to other structured prediction tasks, and to study its synergy with advanced pseudo label and consistency regularization techniques. Finally, we are interested in investigating the theoretical foundations of task-aligned auxiliary learning and its generalization benefits in domain adaptation.

## Conclusion

We propose Masked Feature Modeling (MFM), a novel auxiliary task tailored for unsupervised domain adaptive (UDA) semantic segmentation. Unlike conventional masked image modeling (MIM), MFM operates in feature space, avoiding architectural conflicts and task misalignment. By coupling reconstruction with the pixel-wise classification objective and involving the decoder in auxiliary supervision, MFM strengthens the entire segmentation pipeline.

To support efficient training, we introduce a lightweight Rebuilder module, enabling feature reconstruction without incurring inference-time cost. Extensive experiments across diverse UDA benchmarks and architectures demonstrate the generalizability and effectiveness of our method.

Our findings suggest that task-aligned masked modeling—when designed in feature space and integrated with the segmentation objective—offers a powerful auxiliary signal for domain alignment and decoder supervision. We hope this work broadens the use of masked modeling in domain adaptation and beyond.

## References

- Assran, M.; Duval, Q.; Misra, I.; Bojanowski, P.; Vincent, P.; Rabat, M.; LeCun, Y.; and Ballas, N. 2023. Self-supervised learning from images with a joint-embedding predictive architecture. In *IEEE Conf. Comput. Vis. Pattern Recognit. (CVPR)*, 15619–15629.
- Bao, H.; Dong, L.; Piao, S.; and Wei, F. 2022. Beit: Bert pre-training of image transformers. In *Int. Conf. Learn. Represent. (ICLR)*.
- Bardes, A.; Garrido, Q.; Ponce, J.; Chen, X.; Rabat, M.; LeCun, Y.; Assran, M.; and Ballas, N. 2024. Revisiting feature prediction for learning visual representations from video. *arXiv preprint arXiv:2404.08471*.
- Chen, J.; Chen, C.; Huang, W.; Zhang, J.; Debattista, K.; and Han, J. 2024. Dynamic contrastive learning guided by class confidence and confusion degree for medical image segmentation. *Pattern Recognit. (PR)*, 145: 109881.
- Chen, L.-C.; Zhu, Y.; Papandreou, G.; Schroff, F.; and Adam, H. 2018. Encoder-decoder with atrous separable convolution for semantic image segmentation. In *Eur. Conf. Comput. Vis. (ECCV)*, 801–818.
- Chen, M.; Zheng, Z.; Yang, Y.; and Chua, T.-S. 2023. Pipa: Pixel-and patch-wise self-supervised learning for domain adaptive semantic segmentation. In *ACM Int. Conf. on Multim. (ACM MM)*, 1905–1914.
- Chen, T.; Kornblith, S.; Norouzi, M.; and Hinton, G. 2020. A simple framework for contrastive learning of visual representations. In *Int. Conf. Mach. Learn. (ICML)*, 1597–1607. PMLR.
- Cheng, B.; Misra, I.; Schwing, A. G.; Kirillov, A.; and Girshick, R. 2022. Masked-attention mask transformer for universal image segmentation. In *IEEE Conf. Comput. Vis. Pattern Recognit. (CVPR)*, 1290–1299.
- Cordts, M.; Omran, M.; Ramos, S.; Rehfeld, T.; Enzweiler, M.; Benenson, R.; Franke, U.; Roth, S.; and Schiele, B. 2016. The cityscapes dataset for semantic urban scene understanding. In *IEEE Conf. Comput. Vis. Pattern Recognit. (CVPR)*, 3213–3223.
- Dosovitskiy, A.; Beyer, L.; Kolesnikov, A.; Weissenborn, D.; Zhai, X.; Unterthiner, T.; Dehghani, M.; Minderer, M.; Heigold, G.; Gelly, S.; et al. 2021. An image is worth 16x16 words: Transformers for image recognition at scale. In *Int. Conf. Learn. Represent. (ICLR)*.
- Ghiasi, G.; Lin, T.-Y.; and Le, Q. V. 2018. Dropblock: A regularization method for convolutional networks. *Adv. Neural Inf. Process. Syst. (NIPS)*, 31.
- He, K.; Chen, X.; Xie, S.; Li, Y.; Dollár, P.; and Girshick, R. 2022. Masked autoencoders are scalable vision learners. In *IEEE Conf. Comput. Vis. Pattern Recognit. (CVPR)*, 16000–16009.
- He, K.; Fan, H.; Wu, Y.; Xie, S.; and Girshick, R. 2020. Momentum contrast for unsupervised visual representation learning. In *IEEE Conf. Comput. Vis. Pattern Recognit. (CVPR)*, 9729–9738.
- He, K.; Zhang, X.; Ren, S.; and Sun, J. 2016. Deep residual learning for image recognition. In *IEEE Conf. Comput. Vis. Pattern Recognit. (CVPR)*, 770–778.
- Hoffman, J.; Tzeng, E.; Park, T.; Zhu, J.-Y.; Isola, P.; Saenko, K.; Efros, A.; and Darrell, T. 2018. Cycada: Cycle-consistent adversarial domain adaptation. In *Int. Conf. Mach. Learn. (ICML)*, 1989–1998. Pmlr.
- Hoyer, L.; Dai, D.; and Van Gool, L. 2022. Daformer: Improving network architectures and training strategies for domain-adaptive semantic segmentation. In *IEEE Conf. Comput. Vis. Pattern Recognit. (CVPR)*, 9924–9935.
- Hoyer, L.; Dai, D.; and Van Gool, L. 2024. Domain Adaptive and Generalizable Network Architectures and Training Strategies for Semantic Image Segmentation. *IEEE Trans. Pattern Anal. Mach. Intell. (TPAMI)*, 46(1): 220–235.
- Hoyer, L.; Dai, D.; Wang, H.; and Van Gool, L. 2023a. MIC: Masked image consistency for context-enhanced domain adaptation. In *IEEE Conf. Comput. Vis. Pattern Recognit. (CVPR)*, 11721–11732.
- Hoyer, L.; Dai, D.; Wang, Q.; Chen, Y.; and Van Gool, L. 2023b. Improving semi-supervised and domain-adaptive semantic segmentation with self-supervised depth estimation. *Int. J. Comput. Vis. (IJCV)*, 131(8): 2070–2096.
- Kenton, J. D. M.-W. C.; and Toutanova, L. K. 2019. Bert: Pre-training of deep bidirectional transformers for language understanding. In *NAACL*, volume 1. Minneapolis, Minnesota.
- L. Chen, G. Papandreou, I. Kokkinos, K. Murphy and A. Yuille. 2017. Deeplab: Semantic image segmentation with deep convolutional nets, atrous convolution, and fully connected crfs. *IEEE Trans. Pattern Anal. Mach. Intell. (TPAMI)*, 40(4): 834–848.
- Lee, D.-H.; et al. 2013. Pseudo-label: The simple and efficient semi-supervised learning method for deep neural networks. In *Int. Conf. Mach. Learn. Worksh. (ICMLW)*.
- Lee, G.; Eom, C.; Lee, W.; Park, H.; and Ham, B. 2022. Bi-directional contrastive learning for domain adaptive semantic segmentation. In *Eur. Conf. Comput. Vis. (ECCV)*, 38–55. Springer.
- Li, T.; Roy, S.; Zhou, H.; Lu, H.; and Lathuilière, S. 2023. Contrast, stylize and adapt: Unsupervised contrastive learning framework for domain adaptive semantic segmentation. In *IEEE Conf. Comput. Vis. Pattern Recognit. (CVPR)*, 4869–4879.
- Li, Y.; Mao, H.; Girshick, R.; and He, K. 2022. Exploring plain vision transformer backbones for object detection. In *Eur. Conf. Comput. Vis. (ECCV)*, 280–296. Springer.
- Liao, Y.; Zhou, W.; Yan, X.; Li, Z.; Yu, Y.; and Cui, S. 2024. Geometry-aware network for domain adaptive semantic segmentation. In *Assoc. Advan. Artif. Intell. (AAAI)*, volume 37, 8755–8763.
- Liebel, L.; and Körner, M. 2018. Auxiliary tasks in multi-task learning. *arXiv preprint arXiv:1805.06334*.
- Long, J.; Shelhamer, E.; and Darrell, T. 2015. Fully convolutional networks for semantic segmentation. In *IEEE Conf. Comput. Vis. Pattern Recognit. (CVPR)*, 3431–3440.
- Minaee, S.; Boykov, Y.; Porikli, F.; Plaza, A.; Kehtarnavaz, N.; and Terzopoulos, D. 2021. Image segmentation using deep learning: A survey. *IEEE Trans. Pattern Anal. Mach. Intell. (TPAMI)*, 44(7): 3523–3542.

- Pathak, D.; Krahenbuhl, P.; Donahue, J.; Darrell, T.; and Efros, A. A. 2016. Context encoders: Feature learning by inpainting. In *IEEE Conf. Comput. Vis. Pattern Recognit. (CVPR)*, 2536–2544.
- Richter, S. R.; Vineet, V.; Roth, S.; and Koltun, V. 2016. Playing for data: Ground truth from computer games. In *Eur. Conf. Comput. Vis. (ECCV)*, 102–118. Springer.
- Ronneberger, O.; Fischer, P.; and Brox, T. 2015. U-net: Convolutional networks for biomedical image segmentation. In *MICCAI*, 234–241.
- Ros, G.; Sellart, L.; Materzynska, J.; Vazquez, D.; and Lopez, A. M. 2016. The synthia dataset: A large collection of synthetic images for semantic segmentation of urban scenes. In *IEEE Conf. Comput. Vis. Pattern Recognit. (CVPR)*, 3234–3243.
- Sakaridis, C.; Dai, D.; and Van Gool, L. 2021. ACDC: The adverse conditions dataset with correspondences for semantic driving scene understanding. In *IEEE Int. Conf. Comput. Vis. (ICCV)*, 10765–10775.
- Srivastava, N.; Hinton, G.; Krizhevsky, A.; Sutskever, I.; and Salakhutdinov, R. 2014. Dropout: a simple way to prevent neural networks from overfitting. *J. Mach. Learn. Res. (JMLR)*, 15(1): 1929–1958.
- Tranheden, W.; Olsson, V.; Pinto, J.; and Svensson, L. 2021. Dacs: Domain adaptation via cross-domain mixed sampling. In *WACV*, 1379–1389.
- Tsai, Y.-H.; Hung, W.-C.; Schuler, S.; Sohn, K.; Yang, M.-H.; and Chandraker, M. 2018. Learning to adapt structured output space for semantic segmentation. In *IEEE Conf. Comput. Vis. Pattern Recognit. (CVPR)*, 7472–7481.
- Vaswani, A.; Shazeer, N.; Parmar, N.; Uszkoreit, J.; Jones, L.; Gomez, A. N.; Kaiser, Ł.; and Polosukhin, I. 2017. Attention is all you need. In *Adv. Neural Inf. Process. Syst. (NIPS)*.
- Wang, H.; Tang, Y.; Wang, Y.; Guo, J.; Deng, Z.-H.; and Han, K. 2023. Masked image modeling with local multi-scale reconstruction. In *IEEE Conf. Comput. Vis. Pattern Recognit. (CVPR)*, 2122–2131.
- Wang, M.; and Deng, W. 2018. Deep visual domain adaptation: A survey. *Neurocomputing*, 312: 135–153.
- Wei, C.; Fan, H.; Xie, S.; Wu, C.-Y.; Yuille, A.; and Feichtenhofer, C. 2022. Masked feature prediction for self-supervised visual pre-training. In *IEEE Conf. Comput. Vis. Pattern Recognit. (CVPR)*, 14668–14678.
- Woo, S.; Debnath, S.; Hu, R.; Chen, X.; Liu, Z.; Kweon, I. S.; and Xie, S. 2023. Convnext v2: Co-designing and scaling convnets with masked autoencoders. In *IEEE Conf. Comput. Vis. Pattern Recognit. (CVPR)*, 16133–16142.
- Xie, B.; Li, S.; Li, M.; Liu, C. H.; Huang, G.; and Wang, G. 2023. Sepico: Semantic-guided pixel contrast for domain adaptive semantic segmentation. *IEEE Trans. Pattern Anal. Mach. Intell. (TPAMI)*, 45(7): 9004–9021.
- Xie, E.; Wang, W.; Yu, Z.; Anandkumar, A.; Alvarez, J. M.; and Luo, P. 2021. SegFormer: Simple and efficient design for semantic segmentation with transformers. In *Adv. Neural Inf. Process. Syst. (NIPS)*, 12077–12090.
- Zhang, Z.; Wu, G.; Zhang, J.; Zhu, X.; Tao, D.; and Chai, T. 2025. Unified Domain Adaptive Semantic Segmentation. *IEEE Trans. Pattern Anal. Mach. Intell. (TPAMI)*, 47(8): 6731–6748.
- Zheng, S.; Lu, J.; Zhao, H.; Zhu, X.; Luo, Z.; Wang, Y.; Fu, Y.; Feng, J.; Xiang, T.; Torr, P. H.; et al. 2021. Rethinking semantic segmentation from a sequence-to-sequence perspective with transformers. In *IEEE Conf. Comput. Vis. Pattern Recognit. (CVPR)*, 6881–6890.
- Zhou, W.; and Zhou, Z. 2024. Unsupervised domain adaptation harnessing vision-language pre-training. *IEEE Trans. Circuits Syst. Video Technol. (TCSVT)*.
- Zou, Y.; Yu, Z.; Kumar, B.; and Wang, J. 2018. Unsupervised domain adaptation for semantic segmentation via class-balanced self-training. In *Eur. Conf. Comput. Vis. (ECCV)*, 289–305.